Shot noise in quasi one-dimensional FETs

A.Betti, G. Fiori and G. Iannaccone
Dipartimento di Ingegneria dell'Informazione
Università di Pisa, Via Caruso I-56122 Pisa, Italy
Tel. +39 050 2217639; Fax. +39 050 2217522, email: alessandro.betti,
g.fiori,g.iannaccone@iet.unipi.it

***Abstract*— We propose a novel and general method to investigate shot noise in nanoscale devices by means of Monte Carlo simulations within the self-consistent 3D Poisson-NEGF framework, focusing our attention on Carbon Nanotube and Silicon Nanowire Field effect transistors. We will show that Pauli exclusion principle and Coulomb interactions play an important role in device electrical behavior. In particular, their combined effect leads to a reduction of shot noise in strong inversion down to 23% of the full shot power spectral density for a gate overdrive of 0.4 V.**

I. Introduction

Carbon NanoTube (CNT) and Silicon NanoWire (SNW) FETs have been widely investigated [1] [2] from a performance perspective as promising alternatives to conventional planar MOSFETs. In previous studies however, the figure of merit of their performances has been only concerned with electrical quantities (i.e. I_{on}/I_{off}, sub-threshold swing, transconductance, etc.), while a complete shot noise characterization has been neglected most of the time. Noise is not only critical from an analog and digital design point of view, but it can also provide precious insights into interactions among carriers [3]. Since even in strong inversion only very few electrons take part to transport, nonequilibrium current fluctuations heavily affect the electrical device behavior.

Indeed, since electrons are randomly injected from the reservoirs, the potential barrier along the channel as well as the flow of charge carriers fluctuates in time.

Pauli exclusion principle and Coulomb interactions play an important role in noise analysis. Such effects have been considered for example in double gate MOSFET [4] and in nanoscale ballistic MOSFETs [5], where a very large shot noise suppression, mostly due to Pauli exclusion principle, has been observed.

In order to properly consider such effects, a self-consistent solution of the electrostatics and transport equation is mandatory. To this purpose, we present a new method to compute the power spectral density of shot noise in CNT and SNWFETs based on Monte Carlo simulations of randomly injected electrons from the reservoirs. In particular, our approach is based on the self-consistent solution of the 3D Poisson and Schrödinger equation, within the NEGF formalism. For what concerns CNTs, a p_z tight-binding Hamiltonian has been assumed [6], while an effective mass approximation and an adiabatic decoupling of Schrödinger equation in a set of two-dimensional equations in the transversal plane has been considered for the SNWTs [7]. In both cases, the NEGF transport equation has been solved by means of a mode space approach, since only the lowest subbands take part to transport.

II. Theoretical background

At finite temperatures, the average current along a non-interacting mesoscopic conductor can be expressed as [8]:

$$\langle I \rangle = \frac{2\,e}{h} \sum_n \int T_n(E)\,[f_S(E) - f_D(E)]\,dE \qquad (1)$$

where T_n is the transmission probability of the n-th eigenchannel and it is defined as the n-th eigenvalue of the trasmission probability matrix $t^\dagger t$, while the general expression for the noise spectral density in a two-terminal scattering-free conductor reads [9][10]:

$$S = \frac{2\,e^2}{\pi\hbar} \sum_n \int \{T_n(E)[f_S(E)\,(1 - f_D(E)) + f_D(E)\,(1 - f_S(E)) - T_n(E)\,(f_S(E) - f_D(E))^2]\}\,dE \qquad (2)$$

where f_S and f_D are the Fermi-Dirac occupation factors at the source (S) and drain (D) contacts, respectively. Note that (2) holds only when a constant potential is imposed along the channel, so that Coulomb interaction is completely neglected.

In order to include the effect of Coulomb interaction, transport equation is solved self-consistently with the 3D Poisson equation, while random injection of carriers is modelled by randomizing the occupation factor for states propagating from the source and the drain, as well as the trasmission coefficient. In particular O_{Sm} (O_{Dm}) is the random occupation at source S (drain D) contact for the mode m: it can be either 0 or 1, with a mean value equal to f_S (f_D). Equivalently, we can define the source-to-drain (drain-to-source) trasmission occurrence Ω_{mn} (Ω'_{mn}) from mode n to m, whose mean value is equal to T_{mn} (T'_{mn}), the transmission coefficient from mode n to m. For the CNT-FET structure, the index m and n run along all the transverse modes, the energies and the spin, while for the SNWT structure they also run along the six equivalent minima of the conduction band in the $\mathbf{k}$ space. From a computational point of view, O_{Sm} (Ω_{mn}) is obtained by extracting a random number r with uniform distribution between 0 and 1: if $r < f_S(E)$ ($r < T_{mn}(E)$) then $O_{Sm} = 1$ ($\Omega_{mn} = 1$), otherwise $O_{Sm} = 0$ ($\Omega_{mn} = 0$) (Fig. 1).

Starting from (1), the randomized current can then be expressed as:

$$I = \frac{e\,dE}{2\pi\hbar} \sum_{m\in S} \sum_{n\in D} \left[O_{Sm}\,\Omega_{nm} - O_{Dn}\,\Omega'_{mn}\right] \qquad (3)$$

where dE is the energy step and e is the elementary charge. According to the Milatz Theorem, the power spectrum density S reads

$$S = \frac{2}{\nu}\,var(I) = \frac{4\pi\hbar}{dE}\,var(I) \qquad (4)$$

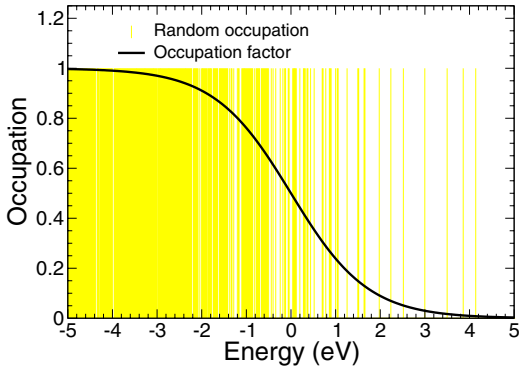

Fig. 1. Random occupation compared to the occupation factor.

where $\nu = dE/(2\pi\hbar)$ is the maximum injection rate of the carriers [10]. The power spectral density can then be obtained by performing simulations on a large ensemble of current samples. We have verified that a record of 500 samples represents a good compromise between computational requirements and accuracy. The variance instead can be expressed as:

$$var\,(I) = \left(\frac{e\,dE}{2\pi\hbar}\right)^2 \{\langle \sum_{\alpha\in S,D}\sum_{n\in\alpha} O^2_{\alpha n}\tau_{\alpha;nn}\,[1-\tau_{\alpha;nn}] - \sum_{\substack{\alpha,\beta\in S,D\\ \beta\neq\alpha}}\sum_{m\in\alpha}\sum_{n\in\beta} O_{\alpha m}O_{\beta n}\gamma^{\beta\leftarrow\alpha}_{nm}\,(1-\tau_{\alpha;mm})\rangle + var(\sum_{m\in S} O_{Sm}\tau_{S;mm} - \sum_{n\in D} O_{Dn}\tau_{D;nn})\} \quad (5)$$

where ($m \in S$, $n \in D$)

$$\gamma^{D\leftarrow S}_{nm} = |t_{nm}|^2_C \quad ; \quad \gamma^{S\leftarrow D}_{mn} = \left|t'_{mn}\right|^2_C = \gamma^{D\leftarrow S}_{nm}$$

and ($l \in S,\ D$)

$$\tau_{\alpha;ll} = \delta_{\alpha S}\ \left(t^\dagger t\right)^C_{ll} + \delta_{\alpha D}\ \left(t'^\dagger t'\right)^C_{ll}$$

Time symmetry has been exploited, since in this work we are only interested in the zero magnetic field case, so that $\left(t'^\dagger t'\right)^C_{ll} = \left(tt^\dagger\right)^C_{ll}$. The index C means that the trasmission probabilities depend on random occupations at both reservoirs.

From a numerical point of view, eq. (4) not only requires the diagonal elements of $t^\dagger t$, but also the elements of the matrix t, for which the computational burden can be high. In order to avoid this issue, imposing identical injected modes from the source and drain reservoirs and $O_{\beta n} = O_{\beta m}\ \forall n \in \beta$, eq. (5) can be further simplified as

$$S = \left(\frac{e^2\,dE}{\pi\hbar}\right)\{\langle \sum_{\alpha\in S,D}\sum_{m\in\alpha} O_{\alpha m}\tau_{\alpha;mm}\,[1-\tau_{\alpha;mm}]\,[O_{\alpha m} - \sum_{\substack{\beta\in S,D\\ \beta\neq\alpha}} O_{\beta m}]\rangle + var(\sum_{m\in S} O_{Sm}\tau_{S;mm} - \sum_{n\in D} O_{Dn}\tau_{D;nn})\} \quad (6)$$

In order to achieve a good trade-off between results and speed, particular attention has also to be posed on the choice of dE. As shown in Fig. 2, $dE = 5\times10^{-4}$ eV provides faster convergence to the Landauer-Büttiker's limit as compared to the other values with a relative error almost equal to 0.16%.

III. Results and Discussions

The simulated devices are depicted in Fig. 3. We consider a (13,0) CNT embedded in SiO_2 with oxide thickness equal to 1 nm, an undoped channel of 10 nm and n-doped CNT extensions 10 nm long, with a molar fraction $f = 5\times10^{-3}$. The SNWT has an oxide thickness equal to 1 nm and the channel length is 10 nm. The wire is undoped and the source and drain extensions (10 nm long) are doped with $N_D = 10^{20}$ cm^{-3}. The device cross section is 4×4 nm^2. In Fig. 4 the transfer characteristics for different V_{DS} are plotted as a function of the gate overdrive. In particular, the threshold voltage V_{th} for the CNT-FET at $V_{DS} = 0.05$ V and 0.5 V is 0.43 V, whereas we obtain a $V_{th} = 0.13$ V for $V_{DS} = 0.5$ V and 0.05 V for the SNW-FET. Current in the CNT-FET transfer characteristics increases for negative gate voltages due to the interband tunneling. Indeed, the larger the negative gate voltage, the higher the number of electrons that tunnel from bound states in the valence band to the drain, leaving positive charge in the channel, which eventually lowers the barrier and increases the off-current [11]. Figs. 5a-b show the semilog plot of the average transfer characteristics computed by performing MC simulations both for CNT and SNWT devices on an ensemble of about 500 current samples: as can be noted, they almost match results obtained by using average occupation factors.

As shown in Fig. 6, only very few electrons are present in the channel, which can make device operation extremely sensitive to charge fluctuations. Furthermore the smaller the drain-to-source voltage, the larger the average number of electrons in the channel, since at low V_{DS} carriers are injected from both contacts.

We now focus on the Fano factor F, defined as the ratio of the computed noise power spectral density S and the so-called full shot noise power spectral density $2q\langle I\rangle$: results are shown in Figs. 7a-b for both CNT and SNW-FET in the saturation

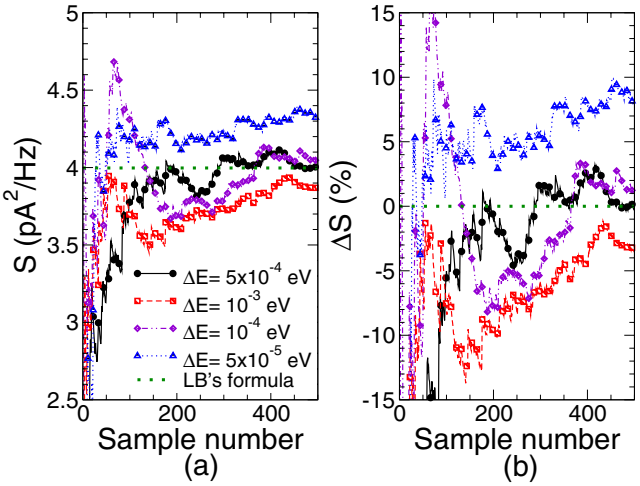

Fig. 2. Noise power spectral density obtained from (6) for a given potential as a function of current sample number for four different energy steps. The simulated structure is a SNWT.

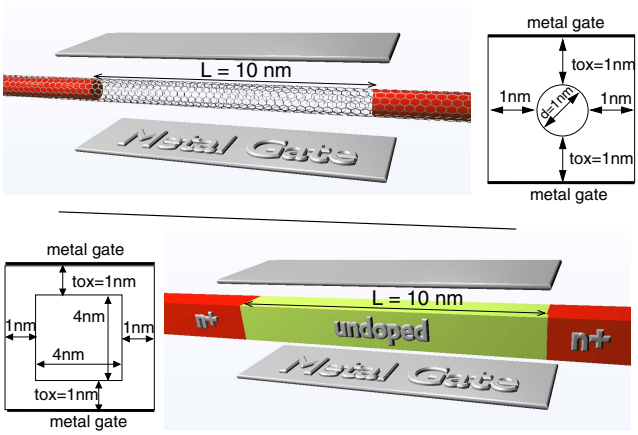

Fig. 3. 3-D structures and transversal cross sections of the simulated CNT-FETs (up) and SNWTs (down).

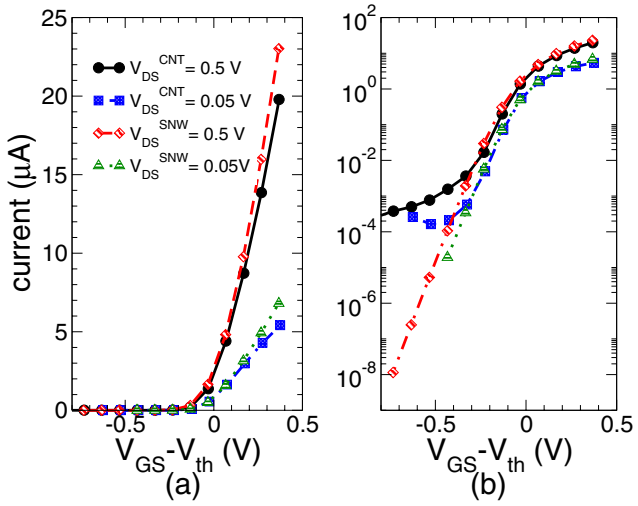

Fig. 4. Transfer characteristics of CNT and SNW-FETs computed for $V_{DS} = 0.05$ V and 0.5 V.

regime. As can be seen, at negative gate voltages, i.e. in the non-degenerate injection limit, drain current noise is very close to $2q\langle I\rangle$. Indeed in sub-threshold regime, Coulomb and Pauli interactions are not effective due the negligible amount of mobile charge in the channel. We can explain such result taking advantage of eq. (2). For energies larger than the top of the barrier, $f_S(E)$ and $f_D(E) \ll 1$ and, since $V_{DS} = 0.5$ V $\approx 19\, k_B T/q$, $f_D(E) \ll f_S(E)$. Moreover for high potential barrier along the channel $T_n(E) \ll 1$, so that we can neglect the second and the third terms of the integrand in (2). The Fano factor then becomes

$$F = \frac{S}{2e\langle I\rangle} \approx \frac{\frac{2e^2}{\pi\hbar}\sum_n \int T_n(E)\, f_S(E)\, dE}{2e\frac{2e}{h}\sum_n \int T_n(E)\, f_S(E)\, dE} = 1 \qquad (7)$$

as we set out to prove. For positive gate voltages instead, the noise is strongly suppressed with respect to the full shot value. In particular, for a 0.4 V overdrive, combined Pauli and Coulomb interactions suppress shot noise down to 23% of the full shot noise. By only including the effect of the Pauli principle, we can instead overestimate shot noise by 180 % for SNWT ($V_{GS} - V_{th} \approx 0.4$ V) and by 70 % for CNT-FET ($V_{GS} - V_{th} \approx 0.3$ V). Fig. 8 shows a distribution of the drain current over 500 random samples obtained by performing MC

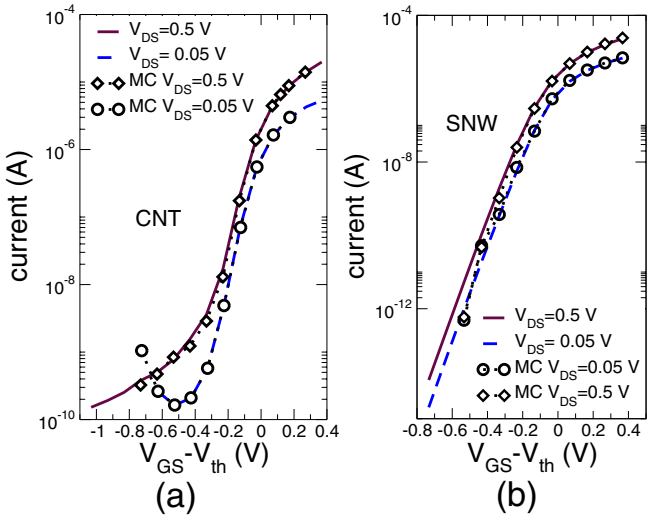

Fig. 5. Average current obtained by MC simulations and by means of continuous Fermi-Dirac statistics for (a) CNT and (b) SNW-FET.

simulations for a CNT-FET, which is reasonably fitted by a Gaussian in the ohmic region ($V_{DS} = 0.05$ V), with a slight asymmetry in the saturation regime ($V_{DS} = 0.5$ V).

Typically, channel noise in FETs is described in terms of a "modified" thermal noise, as $S = \gamma S_T$, where $S_T = 4K_B T g_{d0}$ is the thermal noise power spectrum at $V_{DS} = 0\, V$, and γ is a correction parameter. For a very long channel device, $\gamma = 1$ in the ohmic region and $\gamma = 2/3$ in saturation; for relatively short devices γ practically represents a fitting parameter.

The comparison between shot noise and thermal noise is shown in Fig. 9a for CNTFETs and SNWTs, for different V_{DS} (0.05 and 0.5 V), whereas in Fig. 9b the γ parameter obtained as $\gamma = S/S_T$ is shown. Suppressed shot noise in ballistic one-dimensional FETs out of the equilibrium is relatively close to thermal noise S_T of the channel at the equilibrium. For $V_{DS} = 0.5$ V, S has about the same shape both for CNTFETs and SNWTs, consequently the ratio $\gamma = S/(4k_B T g_{d0})$ is close to one, except in the subthreshold region, where it can be rather large.

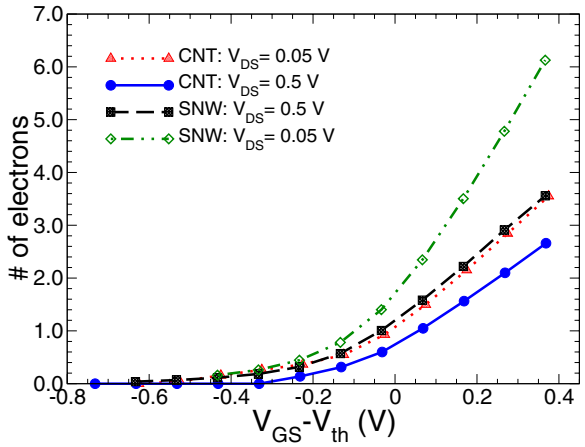

Fig. 6. Average number of electrons in the channel in CNT-FETs and SNW-FETs evaluated for $V_{DS} = 0.05$ V and 0.5 V.

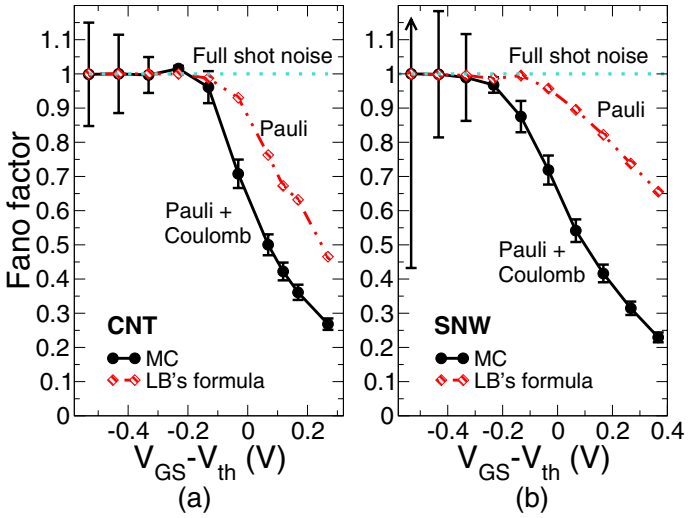

Fig. 7. Fano factor as a function of the gate overdrive $V_{GS} - V_{th}$ for (a) CNT and (b) SNW-FETs. The drain-source voltage V_{DS} is 0.5 V. For $V_{GS} - V_{th} = 0.4$ V, the Fano factor is equal to 0.27 and 0.23 for the CNT and SNW-FETs, respectively.

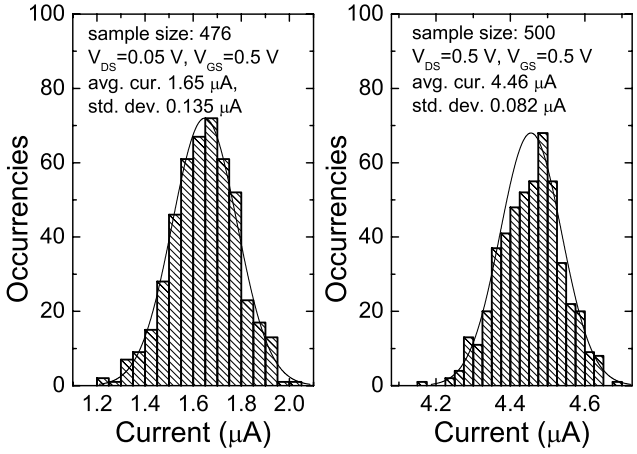

Fig. 8. Current probability density obtained by MC simulations for $V_{GS} = 0.5$ V and (a) $V_{DS} = 0.05$ V and (b) $V_{DS} = 0.5$ V. The simulated structure is a CNT-FET.

IV. Final remarks

We have developed a novel and general approach for the simulation of shot noise in nanoscale devices, which has been applied to one-dimensional FETs (CNT and SNW-FETs). We have shown that Coulomb interaction and Pauli exclusion principle have to be considered and included in a self-consistent Poisson-Schrödinger scheme, in order to quantitively evaluate shot noise. Such effects leads to a large noise suppression above threshold, while full shot noise is observed in the sub-threshold regime.

V. Acknowledgements

This work was supported in part by the EC 7FP through the Network of Excellence NANOSIL (Contract 216171), and by the European Science Foundation EUROCORES Programme Fundamentals of Nanoelectronics, through funding from the CNR (awarded to IEEIIT-PISA) and the EC 6FP, under Project Dewint (Contract ERASCT- 2003-980409).

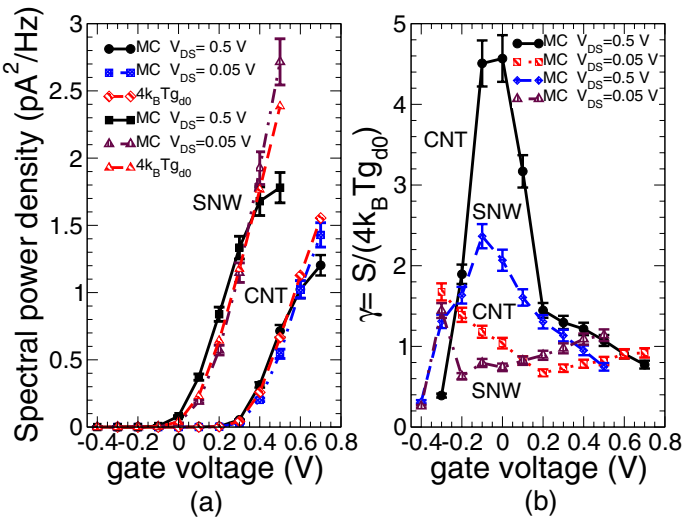

Fig. 9. (a) noise power spectral density obtained by MC simulations and thermal noise density as functions of the gate voltage for CNT and SNW-FETs ($V_{DS} = 0.5$ V, 0.05 V); (b) ratio between the noise power obtained by MC simulations and the thermal noise density as a function of the gate voltage. g_{d0} is the conductance evaluated for $V_{DS} = 0$ V: $g_{d0} = \left(\frac{\partial I_{DS}}{\partial V_{DS}}\right)_{V_{DS}=0}$; k_B is the Boltzmann constant, T is the absolute temperature (300 K).

References

[1] Y. Cui, Z. Zhong, D. Wang, W. U. Wang, C. M. Lieber, "High performance silicon nanowire field effect transistors", *Nano Lett.*, Vol. 3, pp. 149-152, 2003.

[2] J. Guo, A. Javey, H. Dai, M. Lundstrom, "Performance analysis and design optimization of near ballistic carbon nanotube field-effect transistors", *IEDM Tech. Digest*, pp. 703-706, 2004.

[3] G. Iannaccone, G. Lombardi, M. Macucci and B. Pellegrini, "Enhanced Shot Noise in Resonant Tunneling: Theory end Experiment", *Phys. Rev. Lett.* Vol. 80, pp. 1054-1057, 1998.

[4] Y. Naveh, A. N. Korotkov, and K. K. Likharev, "Shot-noise suppression in multimode ballistic Fermi conductors", *Phys. Rev.B*, Vol. 60, pp. R2169-R2172, 1999.

[5] G. Iannaccone, "Analytical and Numerical Investigation of Noise in Nanoscale Ballistic Field Effect Transistors", *J. Comput. Electron.*, Vol. 3, pp. 199-202, 2004.

[6] J. Guo, S. Datta,M. Lundstrom and M. P. Anantam, "Towards Multi-Scale Modeling of Carbon Nanotube Transistors", *Int. J. Multiscale Comput. Eng.*, Vol. 2, pp. 257, 2004.

[7] J. Wang, E. Polizzi, M. Lundstrom,"A three-dimensional quantum simulation of silicon nanowire transistors with the effective-mass approximation", *J. Appl. Phys.*, Vol. 96, pp. 2192-2203, 2004.

[8] Ya. M. Blanter, M. Büttiker, "Shot noise in mesoscopic conductors", *Physics Reports* Vol. 336, pp. 1-166, 2000.

[9] M. Büttiker, "Scattering theory of current and intensity noise correlations in conductors and wave guides", *Phys. Rev.B*, Vol. 46, pp. 12485-12507, 1992.

[10] Xavier Oriols, "Quantum mechanical effects on noise properties of nanoelectronic devices: application to Monte Carlo simulation", *IEEE Transactions on electron devices*, Vol. 50, pp. 1830-1836, 2003.

[11] G. Fiori, G. Iannaccone, G. Klimeck, "A three-dimensional simulation study of the performance of carbon nanotube field-effect transistors with doped reservoirs and realistic geometry", *IEEE Trans. Electron Devices*, Vol. 53, pp. 1782-1788, 2006.